Regular Article

Beam Size Optimization for High-Altitude Platforms to Ground Links in FSO Communications

Dieu Linh Truong[1], **The Ngoc Dang**[2]

[1] School of Information and Communication Technology, Hanoi University of Science and Technology, Vietnam

[2] Department of Wireless Communications, Posts and Telecommunications Institute of Technology, Vietnam

Correspondence: Dieu Linh Truong, linhtd@soict.hust.edu.vn

Communication: received 4 February 2023, revised 27 February 2023, accepted 2 March 2023
Online publication: 1 June 2023, Digital Object Identifier: 10.21553/rev-jec.332
The associate editor coordinating the review of this article and recommending it for publication was Prof. Vo Nguyen Quoc Bao.

***Abstract*– Free-space optical (FSO) communication has been used in practice mainly for short-distance transmission because it requires light of sight (LoS) between the transmitter and receiver. For long-distance communication, to avoid terrestrial obstacles, high-altitude platforms (HAPs) flying at stratosphere are used to carry intermediate FSO transceivers which relay data through several hops from the source to the destination stations. A HAP can communicate with a large ground area if its FSO transceiver projects a wide beam onto the ground. However, an excessively large beam makes the FSO transceiver consume a lot of energy. This study investigates the problem of finding individual optimal beam sizes for FSO transceivers on HAPs so that the total cost of the HAP network, including the amortization, energy, and maintenance costs, is minimized. An optimization algorithm was proposed and implemented. The simulation results show the network designed by the algorithm achieves a nearly optimal number of HAPs, leading to a low network cost.**

***Keywords*– Free Space Optics, High-altitude platform, Beam size optimization, HAP based FSO network.**

1 Introduction

Free-space optical (FSO) communication uses light propagation in free space to transmit data between end-points with clear light of sight (LoS). Commercial FSO transmitters can operate at $1.25 - 10$ Gbps at a distance of $1 - 2$ kilometers [1]. To reach a longer distance, a multi-hop FSO system can be used, where data are transmitted through multiple FSO transceivers [2, 3]. To overcome the lack of LoS between terrestrial FSO devices, researchers proposed using high-altitude platforms (HAPs) to carry intermediate FSO transmitters at altitudes of $17 - 24$ km in the stratosphere. Experimental projects can be cited as Loon Project of Google [4], UAV project of Facebook [5] and Stratobus project of Thales Alenia Space [6].

A communication model using a HAP network is described in [7] and illustrated in Figure 1. According to this model, FSO transceivers on the ground (so call ground FSO nodes) are regrouped into clusters. Each HAP has an FSO transceiver looking down to the ground and is responsible for sending and receiving data to and from the ground FSO nodes of one cluster. This FSO transceiver is called the *serving* FSO. HAPs also carry several FSO transceivers pointing towards each other for inter-HAP communication. These FSO transceivers are called inter-HAP FSO transceivers.

An end-to-end data-switching model for this HAP-based FSO network was also proposed in [7]. A *serving* FSO transceiver manages multiple accesses from the ground nodes of its cluster using the WDM technique; each ground FSO node is assigned a separate wavelength for up and down communication. An IP router regroups IP packets targeting a common cluster into a single flow. A WDM switch is installed on each HAP to route these flows on a wavelength-switched basis over the HAP network. In Figure 1, the blue line illustrates a flow across four HAPs. A flow uses one or more continuous lightpaths between the source and destination HAPs. The number of lightpaths required between a pair of HAPs is determined according to the size of the data flow between them and the transport capacity of a wavelength.

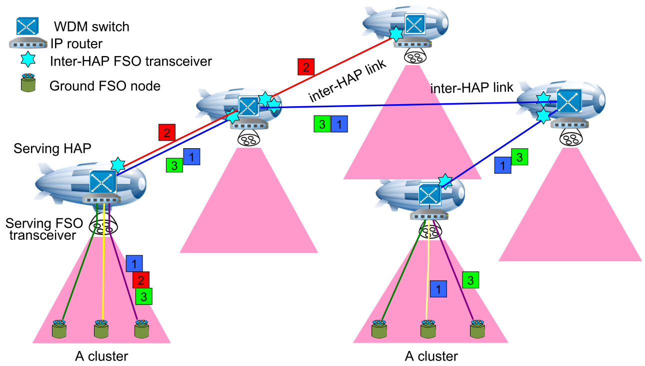

Figure 1. Multi-hop FSO communication system using HAP [7].

In the case of terrestrial FSO transceivers, light beams are usually set to very narrow for low transmitted energy. For multi-hop HAP-based FSO system, a *serving* FSO transceiver must have wide light beam to communicate with distributed ground FSO nodes. Consequently, a *serving* FSO transceiver consumes significantly more energy than a terrestrial FSO transceiver.

A HAP consumes energy for flying and for FSO communications. Solar energy-based HAPs harvest solar energy during the daytime for using during the nighttime. The HAPs can operate continuously in space until they reach to maintenance cycle. Battery energy-based HAPs bring batteries or fuel cells from the ground to use in space, they need to get down once the reserved energy runs out. In this study, we consider that HAPs use only solar energy so that they can work long time in space without lowering down for recharging. The reference solar energy levels are between the minimum harvested at York, UK, which is 42 kWh/day, and at Enugu, Nigeria, which is 290 kWh/day according to the experiments reported in [8].

On the one hand, beam size of a *serving* FSO transceiver is restricted by the available energy. On the other hand, too small beam size leads to more HAPs to be used and thus a costly HAP network. Therefore beam size of *serving* FSO transceivers should be considered carefully for respecting energy limitation and also minimizing the network cost. This research aims to determine an optimal beam size for each *serving* FSO transceiver so that the total investment, energy, and maintenance costs of the HAP network is minimized.

The study in [7] designed a HAP network to cover a set of ground FSO nodes where beam sizes are equal and fixed for all *serving* FSO transceivers. Different to that study, in the current research, individual beam size are tuned for each *serving* FSO transceiver in order to reduce the number of HAPs and thus the HAP network cost. In contrast to the research in [9] that optimizes the inter-HAP beam size, we attempt to optimize the down ground beam size of *serving* FSO transmitters.

The remainder of this paper is organized as follows. Section 2 states the optimization problem that we are trying to solve, the energy consumption model and the energy constraint that leads to the importance of beam size optimization. Section 3 presents an algorithm to solve this problem. Section 4 presents the simulation results. Finally, Section 5 concludes the paper.

2 Problem of Designing Minimal Cost HAP Network and the Role of Beam Optimization

2.1 Problem Statement

The cost of a HAP network contains investment, energy and maintenance costs. We distribute these costs by day as following: 1) daily amortization cost representing investment cost, 2) average maintenance cost per day and 3) daily energy cost. The problem of minimizing the total investment, energy and maintenance costs becomes minimizing the daily cost of the HAP network. The problem is stated as follows:

- Given input parameters including
  - $\mathbb{N}_{\text{FSO}}$: set of ground FSO nodes and their coordinates. The number of nodes in the set is denoted as $|\mathbb{N}_{\text{FSO}}|$.
  - $\mathbb{M}$: data traffic to be carried between ground FSO nodes.
  - ζ_{H}^{day} and ζ_{F}^{day}: daily amortization costs of a HAP and an FSO transceiver on HAP respectively. These costs are defined as the ratio of the prices of the HAP and the FSO transceiver over their expected lifetime duration.
  - ζ^{mtn}: the one-time maintenant cost.
- Outputs to seek are
  - A HAP network with locations of HAPs and individual beam sizes for each *serving* FSO transceiver.
- Optimization objective is
  - Minimizing the daily cost of the HAP network.

Let us introduce additional variables to define daily cost of the HAP network.

- K: Number of HAPs to be used. HAPs are indexed by $i \in 1..K$.
- $n_{\text{FSO}}^{\text{HAP}_i}$: The number of FSO transceivers used on HAP_i for inter-HAP links, excluding the *serving* FSO transceiver.
- $\mathbb{D}^m$: the maintenance cycle of HAPs. Assume that all HAPs has identical cycle.

The overall amortization cost of the network is proportional to the number of HAPs and the number of FSO transceivers. The average maintenance cost per day depends on the maintenance cycle. Solar energy is considered free while the solar panel cost is counted in the amortization cost. As a result, energy cost does not figure explicitly in the total cost. The objective function of minimizing the daily cost of the HAP network becomes

$$\min(K \times \zeta_{\text{H}}^{day} + (K + \sum_{i=1}^{K} n_{\text{FSO}}^{\text{HAP}_i}) \times \zeta_{\text{F}}^{day} + K\frac{\zeta^{mtn}}{\mathbb{D}^m}). \quad (1)$$

The first term in (1) represents the total daily amortization cost of HAPs. The second term is the daily amortization cost of all inter-HAP FSO transceivers and K *serving* FSO transceivers of K HAPs. The last term is the average daily maintenance cost of K HAPs.

2.2 Daily Energy Consumption of a HAP with Payload

This section presents the daily energy consumption of a HAP and the constraint that the HAP needs to respect to rely solely on solar energy. Table I presents the parameters that affect the power consumption of a HAP. Most parameters are set based on industrial experimental projects such as the Loon project [4], Stratobus project [6] and other studies listed in the reference column.

Let us consider the power consumption of a single HAP H_i that has a single *serving* FSO transceiver F_i

Table I
PARAMETERS

Param.	Descriptions	Values	Ref.
	Cost related parameters		
ζ_{H}^{day}	Daily amortization cost of a HAP	100 cost units	
ζ_{F}^{day}	Daily amortization cost of an FSO transceiver on HAP	10 cost units	
ζ^{mtn}	One-time maintenant cost	1000 cost units	
$\mathbb{D}^{m}$	Maintenance cycle	365 days	[6]
	Energy parameters		
$\mathbb{E}^{solar}$	Minimum daily harvested solar energy by a HAP.	42 kWh - 290 kWh	[8]
ρ^{avion}	Power consumed by a HAP to carry a unit of mass	1 W/kg- 2 W/kg	
$\mathbb{P}_{F}^{inter}$	Power consumed by inter-HAP FSO transceivers including 20 W of heating, cooling and management power	20.1 W	[4]
	Inter-HAP FSO link parameters		
C_n^2	Atmosphere structure parameter	$5.0 \times 10^{-18} m^{-2/3}$	
-	Attenuation coefficient	$3.5 \times 10^{-6} m^{-1}$	[4]
-	Coupling loss	45 dBm	
-	Transmitted power of an inter-HAP FSO transceiver	0.1 W	[4]
-	Receiver aperture diameter of an inter-HAP FSO transceiver	0.037 m	[4]
-	Beam width of an inter-HAP FSO transmitter	280 μrad	[4]
	HAP-ground link parameters and variables		
σ	Attenuation coefficient	$3.5 \times 10^{-6} m^{-1}$	
$\mathbb{R}_{rx}$	Receiver aperture radius of a ground FSO transceiver	0.05 m	[1]
$\mathbb{P}_{rx}$	Required received power at a ground FSO transceiver	$7.76.10^{-8}$ W	[4]
	Other parameters		
$\mathbb{H}$	Elevation of HAPs	20 km	
L^{HH}	Maximum length of an inter-HAP link so that its BER is under δ	88 km	
δ	BER threshold for inter-HAP links and lightpaths between HAPs	10^{-3}	
$\mathbb{W}$	The number of wavelengths in WDM technique used on a HAP to ground or inter-HAP link	40; 80	
m_H	Platform mass excluding FSO transceivers	28.5 kg; 500 kg	[4]
m_F	FSO transceiver mass	6.3 kg	[4]

and $n_{\mathrm{FSO}}^{\mathrm{HAP}_i}$ inter-HAP FSO transceivers. The power consumption includes

- $P_{H_i}^{avion}$: Power draw of the avionic part for maintaining HAP H_i with its payload in space.
- $P_{F_i}^{down}$: Transmitted power of the *serving* FSO transceiver of HAP H_i.
- $\mathbb{P}_{F}^{inter}$: Power draw of an inter-HAP FSO transceiver for communication between HAPs. This power draw is fixed equally for all inter-HAP transceiver.

The total daily energy consumption (by 24 hours) of a HAP is

$$\mathbb{E}^{consum} = (P_{H_i}^{avion} + P_{F_i}^{down} + \mathbb{P}_{F}^{inter} \times n_{\mathrm{FSO}}^{\mathrm{HAP}_i}) \times 24. \quad (2)$$

Assuming that $P_{H_i}^{avion}$ is proportional to the weight and ρ^{avion} is the power consumed by the avionic part of the HAP to carry one unit of mass, $P_{H_i}^{avion}$ is expressed by

$$P_{H_i}^{avion} = [m_H + (1 + n_{\mathrm{FSO}}^{\mathrm{HAP}_i}) \times m_F] \times \rho^{avion}, \quad (3)$$

where m_H and m_F are mass of the HAP and a FSO transceiver respectively.

Regarding $P_{F_i}^{down}$, it must be sufficiently large so that all ground nodes served by HAP H_i receive sufficiently strong signals for their detectors. The relationship between $P_{F_i}^{down}$ and the received power at ground node j is defined as

$$\frac{P_j^{rx}}{P_{F_i}^{down}} = e^{-\sigma \times L_j} \times \frac{\mathbb{R}_{rx}^2}{R_i^2}, \quad (4)$$

where

- P_j^{rx} is the received power at ground FSO node j,
- σ is the attenuation coefficient of links between HAPs and ground,
- L_j is the distance between ground FSO node j and its *serving* HAP H_i,
- $\mathbb{R}_{rx}$ is the receiver aperture radius of ground FSO nodes,
- R_i is the ground coverage radius of the *serving* FSO transceiver of HAP H_i. Let α_i be the beam width of the *serving* FSO transceiver of HAP H_i. Then, $R_i = \mathbb{H} \times \tan(\alpha_i/2)$.

In (4), the first term represents the attenuation of laser power through the atmosphere that is described by the exponential Beers-Lambert Law [10]. The second term is the attenuation due to geometric spread.

Referring to Figure 2, we can easily remark that nodes on the border of the ground coverage area of the FSO beam receive the least power because they are the farthest node from the HAP. Therefore, to ensure that all nodes in the coverage area receive sufficient signal, the transmitted power at the *serving* FSO transceiver must be high enough to make the received power at a border node greater than or equal to the required received power threshold. Let us denote this required received power threshold by $\mathbb{P}_{rx}$, then

$$e^{-\sigma\sqrt{R_i^2 + \mathbb{H}^2}} \times \frac{\mathbb{R}_{rx}^2}{R_i^2} \times P_{F_i}^{down} \geq \mathbb{P}_{rx}. \quad (5)$$

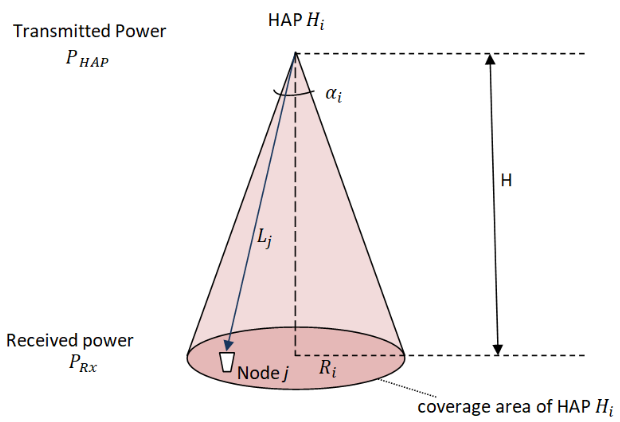

Figure 2. Single beam *serving* FSO transceiver and its footprint.

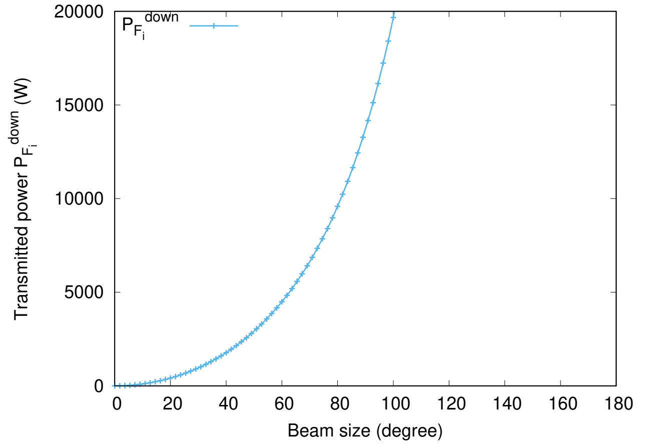

Figure 3. Minimum transmitted power from a *serving* FSO transceiver versus beam sizes according to (6).

In other words, to cover a ground area of radius R_i, the transmitted power from *serving* FSO transceiver F_i should be

$$P_{F_i}^{down} \geq \frac{\mathbb{P}_{rx} \times R_i^2}{e^{-\sigma\sqrt{\mathbb{H}^2+R_i^2}} \times \mathbb{R}_{rx}^2}. \quad (6)$$

Figure 3 illustrates the relationship between beam size α_i and the minimum transmitted power calculated by (6). When the beam size increases from 0° to 180°, the minimum transmitted power increases. To achieve high energy level, multiple lasers could be used in combination with optical amplifiers.

Unlike the links between HAPs and ground nodes, HAP-to-HAP communication is point-to-point; thus, the beam sizes of inter-HAP transceivers can be very small and constant. An inter-HAP link with beam size of 280 μrad, transmitted power of 0.1 W can reaches a distance up to 88 km with a bit error rate (BER) under 10^{-3}. This result is calculated based on the performance analysis of inter-HAP links using on-off keying modulation over Gamma-Gamma atmospheric turbulence channel and link parameters given in Table I. The BER threshold $\delta = 10^{-3}$ is chosen because errors with that BER can be corrected using current Forward Error Correction (FEC) techniques.

Substituting (3) and (6) into (2), we obtain the

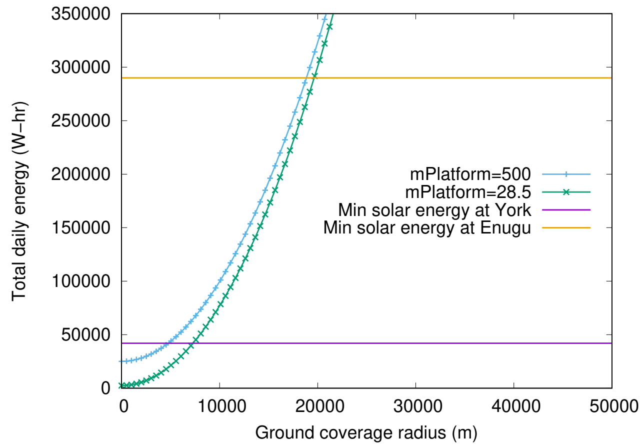

Figure 4. Energy consumption by a HAP when carrying only a *serving* FSO transceiver versus ground coverage radius. $\rho^{avion} = 2$ W/kg.

following formula for the daily energy consumption $\mathbb{E}^{consum}$ of a HAP with payload

$$\mathbb{E}^{consum} = \Bigg((m_H + m_F) \times \rho^{avion} + \frac{\mathbb{P}_{rx} \times R_i^2}{e^{-\sigma\sqrt{\mathbb{H}^2+R_i^2}} \times \mathbb{R}_{rx}^2} + (m_F \times \rho^{avion} + \mathbb{P}_F^{inter}) \times n_{\text{FSO}}^{\text{HAP}_i} \Bigg) \times 24. \quad (7)$$

Figure 4 depicts the total daily energy consumption of a HAP versus ground coverage radius. The energy consumption is calculated by (7) with $n_{\text{FSO}}^{\text{HAP}_i} = 0, \forall i = 1..K$ and $\rho^{avion} = 2$ W/kg. A solar energy level between the minimum harvested at York and Enugu allows a 500 kg HAP covering a ground radius of $5000 - 20000$ meters.

Let denote the daily harvested solar energy by $\mathbb{E}^{solar}$ then the following constraint must be respected by each HAP and its *serving* FSO transceiver.

$$(m_H + m_F) \times \rho^{avion} + \frac{\mathbb{P}_{rx} \times R_i^2}{e^{-\sigma\sqrt{\mathbb{H}^2+R_i^2}} \times \mathbb{R}_{rx}^2} + (m_F \times \rho^{avion} + \mathbb{P}_F^{inter}) \times n_{\text{FSO}}^{\text{HAP}_i} \leq \frac{\mathbb{E}^{solar}}{24}, \quad (8)$$

where $R_i = \mathbb{H} \times \tan(\alpha_i/2)$.

Although the energy constraint (8) is defined for a HAP, the optimal value of coverage radius R_i cannot be computed independently for each HAP because variable $n_{\text{FSO}}^{\text{HAP}_i}$ depends on the topology of the HAP network. In the next section, we propose an algorithm for designing a HAP network topology with optimal beam sizes for *serving* FSO transceivers.

3 Design Solution for Minimal Working Cost HAP Network

In the cost in (1), $\sum_{i=1}^{K} n_{\text{FSO}}^{\text{HAP}_i}$ is actually the total number of FSO transceivers on HAPs, which is twice the number of inter-HAP links. Let denote L^{inter} as the number of inter-HAP links, the cost becomes

$$Cost = K \times (\zeta_{HAP}^{day} + \zeta_{FSO}^{day} + \frac{\zeta^{mtn}}{\mathbb{D}^m}) + 2 \times \text{L}^{inter} \times \zeta_{FSO}^{day}. \quad (9)$$

The problem to solve is to find a HAP network that is capable to carry traffic $\mathbb{M}$, minimizes the cost function (9) while each HAP respects the energy constraint (8). It is clear that the cost is proportional to the number of HAPs and the number of inter-HAP links. We estimate that the daily amortization cost of a HAP is much greater than that of an FSO transceiver; thus, the coefficient $\zeta^{day}_{HAP} + \zeta^{day}_{FSO} + \frac{\zeta^{mtn}}{\mathbb{D}^{m}}$ for K is much greater than the coefficient ζ^{day}_{FSO} for L^{inter}. Consequently, the number of HAPs K should be prioritized to minimize over the number of inter-HAP links L^{inter}. Based on this observation, the topology design is broken in two steps: first, ground nodes are clustered by the smallest number of clusters to minimize K; second, HAPs, which locate at the centres of clusters but at an elevation of 20 km, are interconnected by the fewest number of inter-HAP links. An algorithm designing such a topology has been proposed in [7] where clusters are equal and the cluster radius must be given as an input parameter.

Clustering ground nodes is subject to several constraints such as the maximum number of member nodes per cluster should not exceed $\mathbb{W}$, the radius of the cluster should not violate constraint (8). In addition, the solar energy should not be used entirely for *serving* FSO transceiver to get maximal coverage because the HAP needs some inter-HAP FSO transceivers for communicating with other HAPs. However, the number of inter-HAP FSO transceivers to be used is unknown until the end of the second step. To cope with this, we reserve energy for $\mathbb{V}$ inter-HAP FSO transceivers on each HAP, then identify an initial cluster radius as the maximum one according to the remaining energy. Ground nodes are clustered using that initial cluster radius. Subsequently, an optimization process is performed to enlarge clusters that use fewer inter-HAP FSO transceivers than reserved; and remove some other clusters if possible.

The topology design algorithm is described in Algorithm 1 and is explained below.

- **Find an initial topology with equal cluster radius** First of all, an initial cluster radius is defined as the maximum radius satisfying constraint (8) such that a HAP may have $\mathbb{V}$ inter-HAP links, i.e., $n^{\mathrm{HAP}_i}_{\mathrm{FSO}} = \mathbb{V}$. Then, an initial HAP topology is designed using the algorithm proposed in [7] with that initial cluster radius as the input parameter. The results are a set of clusters of ground FSO nodes $\{S^k\}$, topology $\mathbb{T}$ of the HAP network, and a set of lightpaths $\mathbb{M}^{HAP}$ between HAPs. These lightpaths carry inside them traffic $\mathbb{M}$ between ground nodes. Function Init-Topo($\mathbb{V}$) from Line 26 of Algorithm 1 realizes this step.
- **Optimize beam sizes of *serving* FSO transceivers** Next, we attempt to reduce the number of HAPs in the initial topology by removing unnecessary clusters. A cluster is removable if its ground FSO nodes can be covered by neighboring HAPs and its incoming and outgoing traffic can still be carried by the remaining HAP topology without adding any new links. If some clusters are successfully removed, the resulting topology will have lower cost than the original one. The main steps of the optimization are as follow:
  - Sort clusters by increasing order of their numbers of member ground nodes (Line 3 of Algorithm 1). Test if a cluster is removable from the cluster with the fewest members first. The following testing iteration is applied for each cluster:
    - ∗ Remove all lightpaths in $\mathbb{M}^{HAP}$ that start from, end at or transit through the considering cluster. Remove the HAP corresponding to the cluster from the current topology (Lines 5 to 8 of Algorithm 1).
    - ∗ Reroute the transit lightpath demands over the updated topology (Line 9 of Algorithm 1).
    - ∗ Find another cluster, denoted by S^j, for each ground FSO node f_i of the removing cluster

Algorithm 1: Algorithm to design HAP network with optimal beam size

1: **function** OPTIMIZE-BEAMSIZE
2:   $\mathbb{T} \leftarrow$ INIT-TOPO($\mathbb{V}$)
3:   SORT-CLUSTERS ▷ Sort clusters by nb. of member nodes
4:   **for all** cluster S^k **do** ▷ try to remove S^k
5:     $inoutS^k \leftarrow$ lightpaths start/end at S^k
6:     $transitS^k \leftarrow$ lightpaths transit S^k
7:     $\mathbb{T} - inoutS^k - transitS^k$
8:     $\mathbb{T} \leftarrow \mathbb{T} - H_k$ ▷ Remove HAP k from topo
9:     ROUTE($\mathbb{T}$, $transitS^k$) ▷ Reroute transit lightpaths
10:     **for all** $f_i \in S^k$ **do**
11:       $foundCluster \leftarrow false$
12:       $inoutf_i \leftarrow$ demands from/to f_i
13:       **for all** cluster $S^j \neq S^k$ **do** ▷ try to move f_i to S^j
14:         **if** ENLARGE-C(S^j, f_i) & ROUTE($\mathbb{T}, inoutf_i$) **then**
15:           $S^j \leftarrow S^j \bigcup f_i$ ▷ Move f_i to cluster j
16:           $foundCluster \leftarrow true$
17:           break
18:         **end if**
19:       **end for**
20:       **if** $!foundCluster$ **then**
21:         cluster S^k is not removable
22:       **end if**
23:     **end for**
24:   **end for**
25: **end function**
26: **function** INIT-TOPO($\mathbb{V}$) ▷ Design topo with equal cluster radius
27:   $r \leftarrow$ RMAX($\mathbb{V}$) ▷ calculate initial cluster radius
28:   $\{S^k\} \leftarrow$ Clustering with radius r by algo. in [7]
29:   $\mathbb{M}^{HAP} \leftarrow$ Traffic between HAPs in terms of lightpaths.
30:   $\mathbb{T} \leftarrow$ Design HAP topology by algo. in [7]
31:   **return** $\{S^k\}, \mathbb{T}, \mathbb{M}^{HAP}$
32: **end function**
33: **function** RMAX($n^{\mathrm{HAP}}_{\mathrm{FSO}}$) ▷ function calculates Rmax given the number of FSO devices on a HAP: $n^{\mathrm{HAP}}_{\mathrm{FSO}}$
34: **end function**
35: **function** ROUTE($\mathbb{T}$, demands) ▷ Route demands over topology $\mathbb{T}$ with its current load.
36:   **return** true if routed
37:   **return** false otherwise
38: **end function**

such that the following two conditions are satisfied (Line 14):

1) Ground FSO node f_i is covered by cluster S^j once S^j is enlarged with a radius that respects constraint (8). If HAP H_j uses fewer inter-HAP links than reserved, i.e., $n_{\text{FSO}}^{\text{HAP}_j} \leq \mathbb{V}$, cluster S^j can be enlarged. The HAP may also move towards ground node f_i to avoid a too large radius. The enlarged radius and updated location of the HAP are identified using Algorithm 2.
2) All traffic demands from the ground node f_i are rerouted within the current topology.

* If such a cluster is found, node f_i is moved to cluster S^j and the algorithm continues similarly with remaining ground nodes. Otherwise, the considering cluster is not removable.

Note that, when ground node i joins cluster S^j, its incoming/outgoing traffic is regrouped with the incoming/outgoing traffic of S^j. As a result, $\mathbb{M}^{HAP}$ may change slightly. Nonetheless, node j is moved only when all lightpath demands in the updated $\mathbb{M}^{HAP}$ are well accommodated in the current topology.

Algorithm 2 presents how to enlarge cluster S^j to incorporate ground node f_i. The main idea of the algorithm is to move the centre of S^j towards ground node f_i and enlarge the cluster circle such that it always touches the original one internally (see Figure 5). In so doing, the enlarged cluster still covers all member nodes of the original cluster. Lines 8 to 10 of Algorithm 2 perform this centre movement. The enlarged diameter is always limited by constraint (8) (Line 7 of Algorithm 2).

Algorithm 2: Enlarge cluster S^j for incorporating ground node f_i

1: **function** ENLARGE-C(S^j, f_i)
2: dist $\leftarrow$ distance between the centre of S^j and f_i
3: $maxR_j \leftarrow$ RMAX($n_{\text{FSO}}^{\text{HAP}_j}$)
4: **if** $dist < R_j$ **then** ▷ f_i is covered within S^j.
5: $R_j \leftarrow$ minimum radius to cover member nodes of S^j and f_i
6: **return** true
7: **else if** $dist + R_j < 2 \times maxR_j$ **then** ▷ f_i is covered by H_j with the largest beam size, update S^j centre and radius
8: $S^j.x \leftarrow (S^j.x - f_i.x) \times (\frac{1}{2} + \frac{R_j}{2 \times dist}) + f_i.x$
9: $S^j.y \leftarrow (S^j.x - f_i.x) \times (\frac{1}{2} + \frac{R_j}{2 \times dist}) + f_i.y$
10: $R_j \leftarrow maxR_j$
11: **return** true
12: **else**
13: **return** false ▷ S^j cannot cover f_i
14: **end if**
15: **end function**

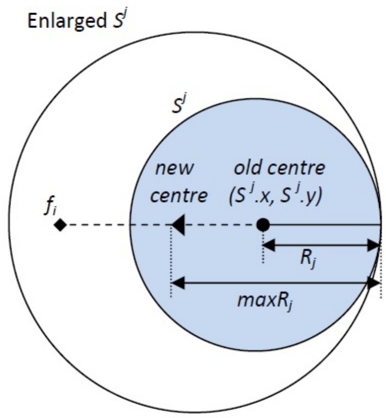

Figure 5. Illustration of Algorithm 2. The original cluster S^j is enlarged and the centre is moved toward f_i. The enlarged cluster touches the original one internally.

4 Simulation Results

The initial topology design using algorithm in [7] and beam size optimization algorithms were implemented. To evaluate the beam size optimization, simulations were performed with parameters in Table I. The cost related values are set up to represent their correlation rather than absolute values, therefore, we do not specify the unit of cost.

A dataset containing 20 test cases was used. Each test case has from 400 to 2800 ground FSO nodes randomly distributed on a square surface of 100 km × 100 km. Test cases with more ground nodes had higher density of ground nodes. The traffic requirement matrix $\mathbb{M}$ contained demands randomly generated between ground FSO nodes such that the total incoming or outgoing traffic of a ground FSO node did not exceed 1 Gbps, which is the capacity of a single wavelength.

The initial topology was designed with $\mathbb{V} = 9$. The initial cluster radius was calculated according to (8) with $n_{\text{FSO}}^{\text{HAP}_i} = \mathbb{V}$. When $\mathbb{E}^{solar}$ varied from 42 to 290 kWh/day, the initial radius varied from 3.646 km to 17.78 km, equivalent to beam widths from 20.66° to 83.27°. Once all the traffic demands in $\mathbb{M}$ were well routed, the initial topology was passed to the beam size optimization process which was completed instantly even for the largest network test case.

Figure 6 shows the footprints of HAPs obtained from the initial topology design with equal beam sizes in sub-figure (a), and after beam size optimization in sub-figure (b), for the test case of 998 ground FSO nodes, $\mathbb{E}^{solar} = 166$ kWh and $\mathbb{W} = 80$. After the beam size optimization, some clusters were slightly enlarged and two HAPs were removed.

4.1 Impact of Solar Energy Level

To determine the impact of the solar energy level, we performed experiments with different daily solar energy levels ranging from 42 to 290 kWh. When $\mathbb{E}^{solar} < 80$ kWh, the algorithms failed to find a topology that accommodated all the demands of $\mathbb{M}$ in most test cases. Therefore, those solar energy levels were excluded from statistics.

Table II shows the results in two groups of $\mathbb{W} = 40$ and $\mathbb{W} = 80$. Each line presents a synthesis of the

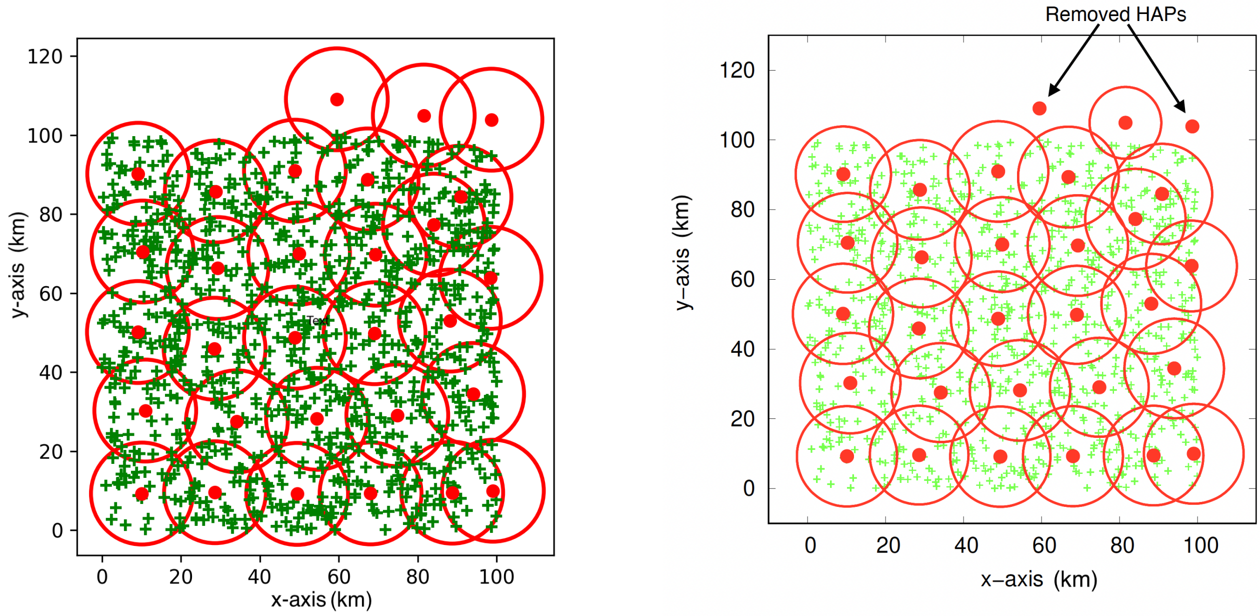

(a) Footprints of HAPs with equal beam sizes

(b) Footprints of HAPs after beam size optimization

Figure 6. Footprints of HAPs (a) obtained from initial topology design with equal beam size and (b) after beam size optimization for set of 998 ground FSO nodes when $\mathbb{E}^{solar} = 166$ kwh, $\mathbb{W} = 80$. A circle represents a cluster. Small points inside a cluster are ground FSO nodes. The dot at the center of a circle is the projected location of a HAP on the ground.

Table II
Results with Different Solar Energy Levels

$\mathbb{E}^{solar}$ (kwh) (1)	Initial radius (km) (2)	K (3)	$\mathbb{L}^{inter}$ (4)	Max. nb. of HAPs removed (5)	Nb. of reduction cases (6)	Max. cost reduction (%) (7)	Cost range (8)
W=40							
100	7.783	47-54	155-184	2	9/13	4.14	8397-9766
130	11.055	34-72	97-319	1	3/20	3.12	5772-14494
150	12.113	30-70	81-313	2	3/20	7.5	5001-14149
166	12.895	25-70	62-310	1	3/20	4.33	4056-14089
180	13.540	24-72	63-323	1	4/20	4.96	4078-14574
200	14.410	24-70	59-308	1	1/20	3.2	3885-14049
240	16.001	18-69	42-302	0	0/20	0	2869-13816
290	17.780	16-69	36-308	0	0/20	0	2532-13936
W=80							
80	7.783	61-75	174-250	2	12/17	3.35	10355-13525
100	9.235	47-59	117-191	3	12/20	5.52	7637-10369
130	11.055	34-42	75-138	2	10/20	5.75	5331-7493
150	12.113	31-36	63-120	1	6/20	4.01	4753-6457
166	12.895	25-40	49-131	2	7/20	6.75	3798-7128
180	13.540	24-40	49-132	1	4/20	4.97	3685-7148
200	14.410	23-36	47-120	1	1/20	4.54	3632-6457
240	16.001	17-37	31-127	1	9/20	6.57	2536-6710
290	17.780	16-35	29-116	1	1/20	3.79	2383-6264

results collected from 20 test cases of the dataset corresponding to a solar energy level. The results in columns 3^{rd}, 4^{th} and 8^{th} are listed in ranges, as they illustrate the variation in values from the smallest test case to the largest test case. When $\mathbb{E}^{solar} = 100$ kWh, $\mathbb{W} = 40$ and $\mathbb{E}^{solar} = 80$ kWh, $\mathbb{W} = 80$, the algorithm failed to find a topology in some large test cases.

We can see that for $\mathbb{W} = 40$ as well as $\mathbb{W} = 80$, when daily solar energy increased, the initial cluster radius increased, the number of HAPs decreased and the number of inter-HAP links decreased. As a result, the absolute cost values (listed in the 8^{th} column) reduced significantly. The optimization process removed up to three HAPs. The 6^{th} column shows the number of

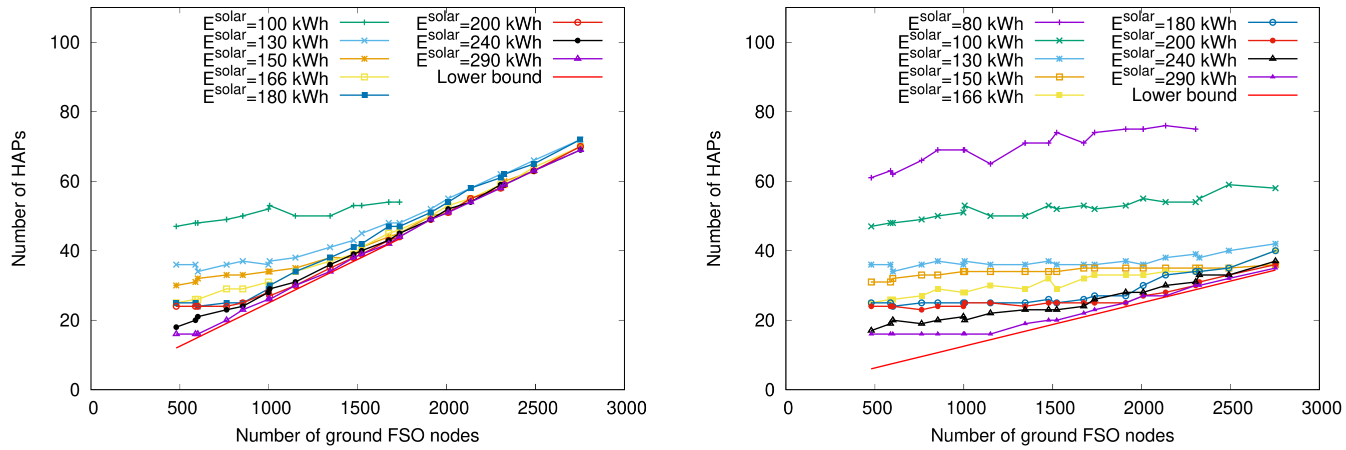

(a) W=40 (b) W=80

Figure 7. Number of HAPs and lower bound with (a) $\mathbb{W} = 40$ and (b) $\mathbb{W} = 80$ in different solar energy levels.

test cases, where the optimization process successfully removed at least one HAP, over the total number of test cases. These values demonstrate that the optimization process removed fewer HAPs and less often when the energy level went up. The explanation is that, to remove a cluster, other clusters needed to widen to cover the ground nodes of the former. To enlarge the coverage, a HAP traded off some of its inter-HAP links (used fewer inter-HAP links than $\mathbb{V}$), but the power gained from this trading may not be sufficient to expand its cluster to cover neighboring ground nodes. This happened mostly with large clusters because the power consumption of a *serving* FSO transceiver increases exponentially with its radius coverage.

Although higher solar energy level helps reduce the absolute network cost, the reduction becomes slower when the energy level is already high. Indeed, with $\mathbb{W} = 80$, when $\mathbb{E}^{solar}$ passed from 80 to 130 kWh, the network cost, number of HAPs and number inter-HAP links reduced almost 50%. However, from 240 to 290 kWh, there is also a 50 kWh difference, but the network cost, number of HAPs and number of inter-HAP links reduced less than 10%. We remark that, $\mathbb{E}^{solar} \geq 130$ kWh seems to be sufficient to avoid expensive HAP networks with $\mathbb{W} = 80$.

4.2 Number of HAPs

According to the numbers in the 5^{th} column of Table II, more HAPs were removed by the optimization process with lower solar energy. When $\mathbb{E}^{solar} \geq 180$ kWh, the optimization process removed maximally one HAP and even none in many cases. To determine whether the number of HAPs could be reduced further, we compared the number of HAPs after optimization against a lower bound. Since each HAP cannot serve more than $\mathbb{W}$ ground FSO nodes, a lower bound number of HAPs is

$$n_{\text{HAP}}^{LB} = \frac{|\mathbb{N}_{\text{FSO}}|}{\mathbb{W}}, \qquad (10)$$

where $|\mathbb{N}_{\text{FSO}}|$ is the number of ground FSO nodes.

Figure 7 shows the number of HAPs obtained with different solar energy levels and the lower bound when (a) $\mathbb{W} = 40$ and (b) $\mathbb{W} = 80$. With $\mathbb{W} = 40$ and $\mathbb{E}^{solar} \geq 130$ kWh, the number of HAPs approached closely with the lower bound starting from test cases with 1000 ground nodes or more. With $\mathbb{W} = 80$, $\mathbb{E}^{solar} \geq 180$ kWh, the number of HAPs approached also the lower bound from 1500 ground nodes. This means the number of HAPs is close to the optimal value. That also explains why the optimization process could not remove more than one HAP with greater $\mathbb{E}^{solar}$.

Finally, the fact that the optimization process removed very few HAPs, while the final numbers of HAPs were close to the optimal values, reveals that the initial cluster radius was well chosen.

4.3 Number of inter-HAP Links

Figure 8 illustrates the number of inter-HAP links with different solar energy levels. The number of inter-HAP links clearly reduced when the wavelength density increased from $\mathbb{W} = 40$ to $\mathbb{W} = 80$. In other words, using higher DWDM technique helps to reduce the number of inter-HAP FSO transceivers and thus network cost.

Table III presents the detailed results of a single solar energy level $\mathbb{E}^{solar} = 166$ kWh, the middle value of the testing $\mathbb{E}^{solar}$ range. Columns 4^{th} and 8^{th} show that the number of inter-HAP links decreased after the optimization process because few inter-HAP links were removed along with every removal of HAPs.

4.4 Impact of Optimization Process on Cost Reduction

Values in column 7^{th} of Table II show that up to 7.5% cost reduction was obtained thanks to the optimization process. Values in column 6^{th} reveal that the optimization process performed better with $\mathbb{W} = 80$ than with $\mathbb{W} = 40$ because it eliminated HAPs more frequently. In general, a better cost reduction was obtained with $\mathbb{W} = 80$. Nonetheless, the values in the 7^{th} column points out that the best cost reduction, 7.5%, was reached with $\mathbb{W} = 40$.

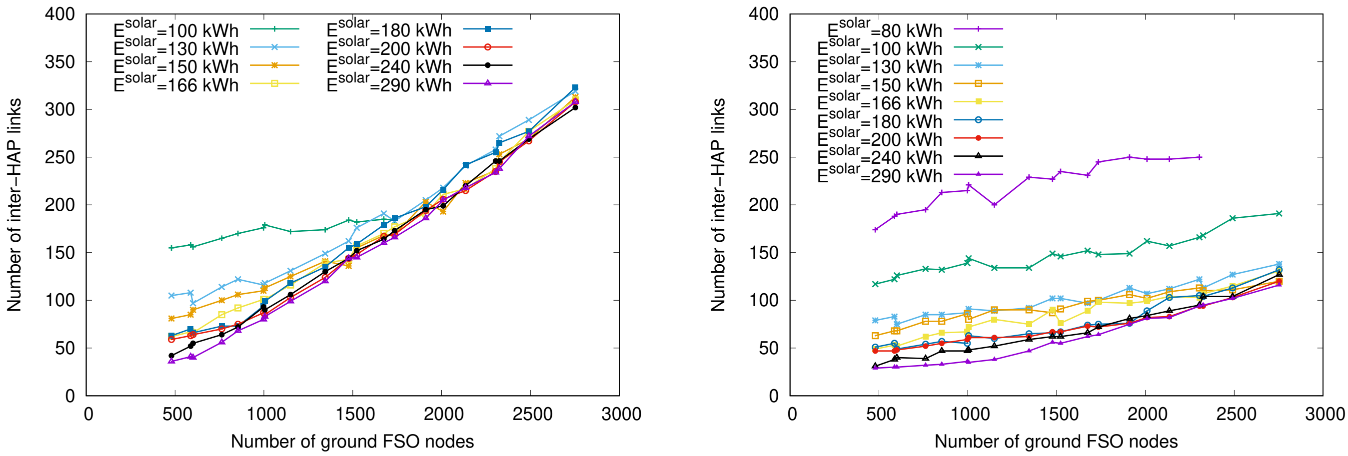

(a) W=40 (b) W=80

Figure 8. Number of inter-HAP links when (a) $\mathbb{W} = 40$ and (b) $\mathbb{W} = 80$ for different solar energy levels.

Table III
Results with Different Numbers of Ground FSO Nodes when $\mathbb{E}^{solar} = 166$ kWh.

	W=40				W=80			
$\lvert\mathbb{N}_{FSO}\rvert$ (1)	K (2)	Nb. of removed HAPs (3)	Nb. of inter-HAP link reduced (4)	Reduced cost (%) (5)	K (6)	Nb. of removed HAPs (7)	Nb. of inter-HAP link reduced (8)	Reduced cost (%) (9)
480	25	0	0	0	25	0	0	0
588	26	1	3	3.89	26	1	4	4.61
601	26	1	4	4.34	26	1	4	4.63
763	29	0	0	0	27	0	0	0
854	29	0	0	0	29	0	0	0
998	31	0	0	0	28	2	5	6.75
1005	30	0	0	0	28	0	0	0
1150	34	0	0	0	30	0	0	0
1345	37	0	0	0	29	1	3	3.5
1477	39	0	0	0	32	0	0	0
1523	41	0	0	0	29	1	3	3.48
1675	45	0	0	0	32	1	4	3.45
1736	46	0	0	0	33	0	0	0
1911	50	0	0	0	33	1	4	3.29
2009	53	0	0	0	33	0	0	0
2135	55	0	0	0	34	0	0	0
2304	59	0	0	0	34	0	0	0
2325	59	1	9	2.47	34	0	0	0
2491	64	0	0	0	35	0	0	0
2753	70	0	0	0	40	0	0	0

Columns 5^{th} and 9^{th} of Table III present the percentage of network cost reduction when daily solar energy was 166 kWh. There is no clear relationship between cost reduction and the number of ground nodes but it seems that a smaller cost reduction was obtained with a large number of ground nodes.

5 Conclusions and Future Works

In this study, we focused on finding the optimal beam sizes for *serving* FSO transceivers on HAPs. The beam size of a *serving* FSO transceiver is restricted by the amount of solar energy available on a HAP and the number of inter-HAP FSO transceivers communicating with other HAPs. We proposed a method to calculate the initial beam size based on (8). Then, we proposed an optimization process that adjusts the beam sizes of *serving* FSO transceivers individually according to the actual energy usage of the corresponding HAPs. The experiment results showed that the initial beam size was well chosen such that with a small or even zero improvement by the optimization process, the numbers of HAPs in the designed networks were close to the optimal. Although the optimization process did not make a consistent improvement in all test cases, it allowed a reduction of up to 7.5% in the total network cost. In addition, the optimization process is not costly in terms of computational resources and running time.

In this study, a HAP employs a single serving FSO transceiver. In the future, we intend to consider multiple serving FSO transceivers on a single HAP. Each serving FSO transceiver should be directed to the ground at an individual angle; thus, multiple serving FSO transceivers together cover a much wider ground area. We expect that the number of HAPs will be substantially reduced leading to a further reduction in network cost.

Acknowledgment

This research was funded by the Vietnam National Foundation for Science and Technology Development (NAFOSTED) under grant number 102.02-2018.305.

References

[1] fSONA, "SONABeam 2500-E+ model specifications," http://fsona.com, accessed Jan. 2022.
[2] A. Acampora and S. Krishnamurthy, "A broadband wireless access network based on mesh-connected free-space optical links," *IEEE Personal Communications*, vol. 6, no. 5, pp. 62–65, 1999.
[3] J. Zhang, "Proposal of free space optical mesh network architecture for broadband access," in *Proceedings of the IEEE International Conference on Communications. ICC 2002 (Cat. No.02CH37333)*, vol. 4, 2002, pp. 2142–2145.
[4] B. Moision, B. Erkmen, E. Keyes, T. Belt, O. Bowen, D. Brinkley, P. Csonka, M. Eglington, A. Kazmierski, N. hyong Kim, J. Moody, T. Tu, and W. Vermeer, "Demonstration of free-space optical communication for long-range data links between balloons on Project Loon," in *Free-Space Laser Communication and Atmospheric Propagation XXIX*, H. Hemmati and D. M. Boroson, Eds., vol. 10096, International Society for Optics and Photonics. SPIE, 2017, pp. 259 – 272.
[5] C. Chen, A. Grier, M. Malfa, E. Booen, H. Harding, C. Xia, M. Hunwardsen, J. Demers, K. Kudinov, G. Mak, B. Smith, A. Sahasrabudhe, F. Patawaran, T. Wang, A. Wang, C. Zhao, D. Leang, J. Gin, M. Lewis, D. Nguyen, and K. Quirk, "High-speed optical links for UAV applications," in *Free-Space Laser Communication and Atmospheric Propagation XXIX*, H. Hemmati and D. M. Boroson, Eds., vol. 10096, International Society for Optics and Photonics. SPIE, 2017, pp. 316 – 324.
[6] Thales group, "What's up with stratobus," https://www.thalesgroup.com/en/worldwide/space/news/whats-stratobus, 2017, accessed Jan. 2022.
[7] D. L. Truong, X. V. Dang, and T. N. Dang, "Survivable free space optical mesh network using high-altitude platforms," *Optical Switching and Networking*, vol. 47, p. 100716, 2023.
[8] S. C. Arum, D. Grace, P. D. Mitchell, M. D. Zakaria, and N. Morozs, "Energy management of solar-powered aircraft-based high altitude platform for wireless communications," *Electronics*, vol. 9, no. 1, 2020.
[9] V. V. Mai and H. Kim, "Beam size optimization and adaptation for high-altitude airborne free-space optical communication systems," *IEEE Photonics Journal*, vol. 11, no. 2, pp. 1–13, 2019.
[10] A. A. Farid and S. Hranilovic, "Outage capacity optimization for free-space optical links with pointing errors," *Journal of Lightwave Technology*, vol. 25, no. 7, pp. 1702–1710, 2007.

Dieu Linh Truong is currently an associate professor in Faculty of Computer Engineering, School of Information and Communication Technology, Hanoi University of Science and Technology, Vietnam. She received her PhD from the Department of Computer Science and Operations Research, University of Montreal, Canada, in 2007. She was visiting scholar at the University of Aizu, Japan in 2010, at Oklahoma State University, USA in 2012-2013, and at Grenoble Institute of Technology, France in 2019. Her interests include optical networks, and survivable network routing and design problems.

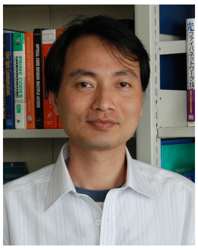

The Ngoc Dang is an associate professor/vice dean of Faculty of Telecommunications and head with the Department of Wireless Communications at Posts and Telecommunications Institute of Technology, Vietnam. He was also an invited researcher at FOTON ENSSAT Lab., Universite de Rennes 1, (France) and a research fellow at Computer Communications Lab., the University of Aizu (Japan). His current research interests include the area of communication theory with a particular emphasis on modeling, design, and performance evaluation of optical CDMA, RoF, QKD, and optical wireless communication systems. He is a member of IEEE.